Improving satellite monitoring of coastal inundations of pelagic Sargassum algae with wind and citizen science data

Nathan F. Putman [a,*], R. Taylor Beyea [a], Lowell Andrew R. Iporac [b], Joaquin Triñanes [c,d,e], Emilie G. Ackerman [a], Maria J. Olascoaga [f], Christian M. Appendini [g], Jaime Arriaga [h], Ligia Collado-Vides [b], Rick Lumpkin [c], Chuanmin Hu [i], Gustavo Goni [c]

[a] LGL Ecological Research Associates, Bryan, TX 77802, USA
[b] Department of Biological Sciences Institute of Environment, Florida International University, Miami, FL 33199, USA
[c] Atlantic Oceanographic and Meteorological Laboratory, National Oceanic and Atmospheric Administration, Miami, FL 33149, USA
[d] Department of Electronics and Computer Science, Universidade de Santiago de Compostela, Santiago 15782, Spain
[e] Cooperative Institute for Marine and Atmospheric Studies, Rosenstiel School of Marine and Atmospheric Science, University of Miami, Miami, FL 33149, USA
[f] Department of Ocean Sciences, Rosenstiel School of Marine, Atmospheric and Earth Science, University of Miami, Miami, FL 33149, USA
[g] Laboratorio de Ingeniería y Procesos Costeros, Instituto de Ingeniería, Universidad Nacional Autónoma de México, Sisal, Mexico
[h] Faculty of Civil Engineering and Geosciences, Delft University of Technology, 2628 CN Delft, the Netherlands
[i] College of Marine Science, University of South Florida, St. Petersburg, FL 33701, USA

ARTICLE INFO

ABSTRACT

Massive blooms of pelagic Sargassum algae have caused serious problems to coastal communities and ecosystems throughout the tropical Atlantic, Caribbean Sea, and Gulf of Mexico since 2011. Efforts to monitor and predict these occurrences are challenging owing to the vast area impacted and the complexities associated with the proliferation and movement of Sargassum. Sargassum Inundation Reports (SIRs) were first produced in 2019 to estimate the potential risk to coastlines throughout the Intra-American Sea at weekly intervals at 10 km resolution. SIRs use satellite-based data products to estimate beaching risk from the amount of offshore Sargassum (quantified by a Floating Algal density index). Here we examine whether including wind metrics improves the correspondence between the offshore Floating Algal density index and observations of Sargassum along the coastline. For coastal observations, we quantified the percent coverage of Sargassum in photos obtained from the citizen science project "Sargassum Watch" that collects time-stamped, georeferenced photos at beaches throughout the region. Region-wide analyses indicate that including shoreward wind velocity with SIR risk indices greatly improves the correspondence with coastal observations of Sargassum beaching compared to SIR risk indices alone. Site-specific analyses of photos from southeast Florida, USA, and data from a continuous video monitoring study at Puerto Morelos, Mexico, suggest potential uncertainties in the suite of factors controlling Sargassum beaching. Nonetheless, the inclusion of wind velocity in the SIR algorithm appears to be a promising avenue for improving regional risk indices.

1. Introduction

For more than a decade, massive amounts of pelagic Sargassum, a floating macroalgae, have swept through the tropical Atlantic into the western Atlantic, Caribbean Sea, and the Gulf of Mexico (Franks et al., 2016; Wang et al., 2019). These seasonal blooms of Sargassum have led to unprecedented inundation of coastlines throughout the region resulting in a suite of environmental, economic, and human health problems (Devault et al., 2021; Oxenford et al., 2021). Problems range

from disrupting fishing and boat navigation to accumulating arsenic and heavy metals in coastal areas as they leach from Sargassum's tissue during decomposition (Hu et al., 2016; Dassié et al., 2022; Ortega-Flores et al., 2022; Rodriguez-Martinez et al., 2022). Monitoring and forecasting Sargassum beaching events are necessary to improve mitigation and clean-up responses, work towards long-term adaptive management operations, and provide information to the growing entrepreneurial community attempting to valorize these influxes of Sargassum (Lopez Miranda et al., 2021; Oxenford et al., 2021). The widespread nature of

---

this phenomenon presents significant challenges for efforts to synoptically monitor coastal inundations (Maréchal et al., 2017; Johnson et al., 2020; Bernard et al., 2022). The application of satellite-based sensors with the capability of detecting Sargassum from space has been used to develop monitoring tools, such as the Sargassum Inundation Reports (SIRs) produced by the National Oceanographic and Atmospheric Administration (NOAA) Atlantic Oceanographic and Meteorological Laboratory (AOML). The SIRs provide weekly assessments of inundation risk to coastlines throughout the Intra-American Sea from 2019 to present (Triñanes et al., 2021).

The SIR risk estimates are based on data from the Alternative Floating Algal Index (AFAI), which quantifies the magnitude of red-edge reflectance of vegetation on the ocean surface using data derived from the Moderate Resolution Imaging Spectroradiometer (MODIS) on the *Terra* and *Aqua* satellites and the Visible Infrared Imaging Radiometer Suite (VIIRS) on the *Suomi National Polar-orbiting Partnership* (*S-NPP*) satellite (Wang and Hu, 2016, 2018). A Floating Algae (FA) density index is computed from the AFAI at a resolution of $0.1°$ (~10 km), applying a mask over coastal waters 0–30 km from the shore due to unreliability of floating algae estimates in nearshore areas. Such FA density maps have been made available in near real-time through the Sargassum Watch System (SaWS, Hu et al., 2016; https://optics.marine.usf.edu/projects/saws.html). The SIR algorithm then calculates an "inundation potential" or "risk" for coastlines using 7-day composites of the FA density index within a 50 km radius of each location (thus inundation potentials are based on FA densities between 30 and 50 km from shore). Inundation potentials are assigned as Low (< 0.05% FA density), Medium (0.05 – 0.2%), and High (> 0.2%) (Triñanes et al., 2021). This product is made freely available at: https://www.aoml.noaa.gov/phod/sargassum_inundation_report/.

While these estimates provide an indication of the amount of Sargassum within the vicinity of the coastline, they do not assess how these risk values correspond to actual beaching (Triñanes et al., 2021). This is due to two primary reasons: uncertainties in the satellite-based Sargassum estimates and lack of physical driving mechanisms in the

SIR algorithm. Specifically, the algorithms used in estimating Sargassum amount in a given location are based on medium-resolution (~ 1 km per image pixel) satellite data that do not work well in nearshore waters because benthic habitats (e.g., seagrass, coral reefs, hard bottom) often lead to high AFAI values that are misinterpreted as being from floating algae. On the other hand, the medium-resolution satellite data may miss small Sargassum mats, leading to possible underestimates of Sargassum amounts (Ody et al., 2019). Therefore, a 30-km nearshore mask was used to avoid misinterpretation. Additionally, factors influencing the probability of Sargassum remaining offshore or moving onshore are not incorporated into the present SIR algorithm. Pelagic Sargassum is positively buoyant, and its movement is driven by physical processes occurring near the ocean surface. Winds contribute to near-surface currents and waves and directly transfer momentum to objects, like Sargassum, that extend above the ocean surface (Miron et al., 2020). The importance of wind on Sargassum movement has been shown at the scale of tracking trajectories of individual mats (Putman et al., 2020), accounting for its distribution at the ocean basin scale (Berline et al., 2020; Beron-Vera et al., 2022) and its seasonal cycle of growth, dispersal, and mortality (Putman and Hu, 2022). Winds likely play an important role in the movement of Sargassum from offshore to coastal areas, and considering wind effects could be an important component for improving inundation risk assessments.

To compare SIR estimates of inundation risk to conditions observed at the coastline, we make use of in situ data collected by two monitoring programs of beached Sargassum (Rutten et al., 2021; Iporac et al., 2022; Fig. 1). The two monitoring programs differ in scale, methodology, and purpose. Iporac et al. (2022) opportunistically obtain photos from citizen scientists at beaches across much of the region monitored by SIRs (Iporac et al., 2022). Rutten et al. (2021) use highly standardized continuous video monitoring of Sargassum beaching at a single site in Puerto Morelos in Quintana Roo, Mexico. These ground-truthing methods benefit from a consistent, local-scale monitoring of a site that can confirm the presence and intensity of Sargassum. Previous programs were adept in detecting algal blooms and influxes, such as of pelagic
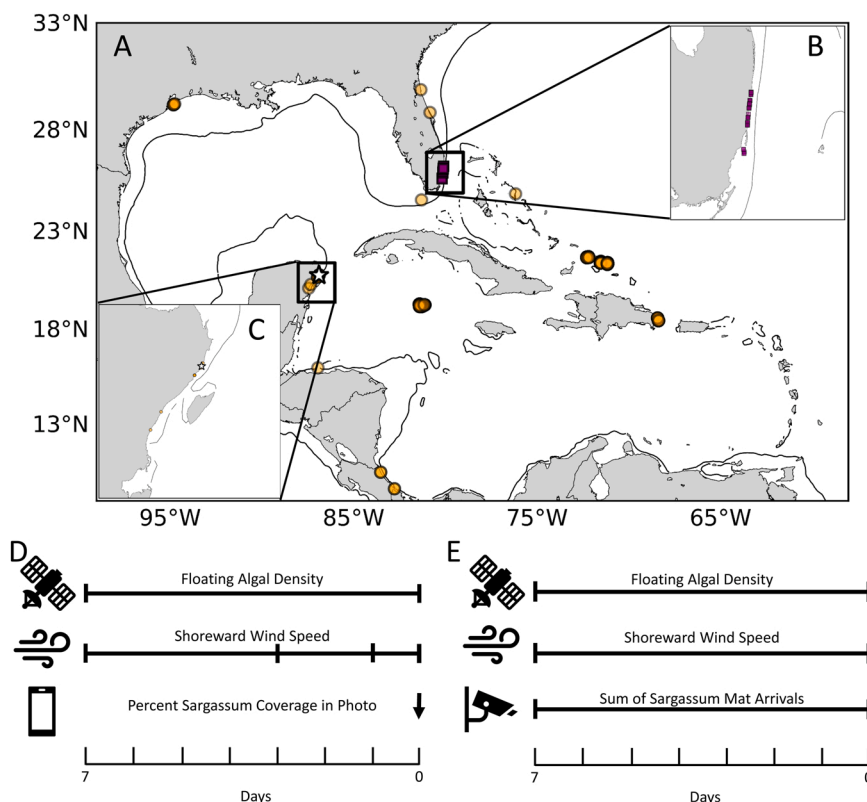
Fig. 1. Locations of observations used to assess the relationship between satellite-derived Floating Algal (FA) densities used in Sargassum Inundation Reports (SIR) and conditions at the coast. Maps are Mercator projections, north is upward. (A) Orange circles correspond to locations of citizen science photos used in the region-wide analyses (n = 436 sites), (B) purple squares show locations of citizen science photos used in analyses for southeast Florida, USA (n = 219 sites), and (C) the white star indicates the location of Puerto Morelos, Quintana Roo, Mexico where continuous video monitoring of incoming *Sargassum* mats was obtained (n = 97 weeks). (D) For the regional and southeast Florida citizen science datasets, FA density was based on a 7-day composite and wind metrics (mean, maximum, and minimum shoreward velocity) were taken over 1, 3, and 7 days prior to the photo date. (E) For the continuous video monitoring data set from Quintana Roo, the mat counts, FA density, and wind metrics were taken over the same 7-day period.

Sargassum (Arellano-Verdejo and Lazcano-Hernández, 2021, Triñanes et al., 2021, Valentini and Balouin, 2020), Didymo blooms (Gillis et al., 2018), and harmful phytoplankton blooms (Cunha et al., 2017). The efficacy of the citizen science programs however varies by the commitment and training levels of the volunteers (Iporac et al., 2020), the spatial and temporal variability of data collected (Geldmann et al., 2016, Millar et al., 2019, Nerbonne et al., 2008), and the large output of data that would need processing for further analyses (Iporac et al., 2022).

Here, we quantified the amount of Sargassum observed by the monitoring programs (either percent coverage in photos (Iporac et al., 2022) or the number of mats detected per week by video (Rutten et al., 2021)) and correlated them with the corresponding FA density index used in the SIR risk assessments. We then tested whether the inclusion of different metrics of shoreward wind speed would strengthen the correlation between offshore FA density and observations at the coast. From these analyses, we contribute to a better understanding of the interaction between pelagic Sargassum and the environment, specifically the role of wind in moving Sargassum from offshore into coastal areas. With this new information we present recommendations for including wind data in future implementations of SIRs or other schemes to refine inundation risk estimates.

2. Methods

2.1. Observations of sargassum along the coast

We obtained a database of photos from the citizen science project "Sargassum Watch" (https://five.epicollect.net/project/sargassum-watch). The purpose of this database is to collect and store photographs taken by individuals at locations along the coastline to capture presence and inundation magnitude of beached Sargassum. The methodology and data are described in detail in Iporac et al. (2022). Using their smartphone camera, oriented vertically, citizen science participants are requested to upload 3 photos taken standing at the shoreline with one to the left, one to the center, and one to the right. Date, latitude, and longitude were recorded for photos; additionally, participants could include information such as the type of Sargassum, its condition (e.g., mostly fresh, mostly decomposed, or a mix), and whether there was evidence of site cleaning. The photos and associated data were uploaded to Epicollect5 by networks of committed volunteers to consistently monitor selected sites, and volunteers were given standardization protocols and training sessions (in-person or online) to use the smartphone app if the volunteer or group requested (Iporac et al., 2022). For the years examined in this work (2019–2021), the Epicollect5 database contained more than 4000 unique date/locations at coastlines throughout the Caribbean Sea, Gulf of Mexico, east coast of Florida, and the Bahamas. These photos were unevenly distributed across space and through time, with more than 60% occurring in southeast Florida. So as not to bias results of a region-wide assessment to a single area, we separated the photos taken in southeast Florida to use in separate region-wide and site-specific analyses described below.

2.1.1. Region-wide dataset

For the region-wide analysis (Fig. 1A), photos were selected based on whether FA density and wind data were available for comparison at the corresponding location and date (Fig. 2). Photos without both FA density and wind data were excluded from analysis. Where data were available, we randomly selected either the left or right photo for analysis at each site (n = 436). In cases where the visibility or orientation of the randomly selected photo was compromised (e.g., blurry, improper direction of camera), we selected the other or removed the sample altogether if neither photo complied with the protocol. Each photo was vertically cropped to remove the sky, then 50 points were randomly overlayed across the photo using Coral Point Count with Excel extensions software (CPCe) (Kohler and Gill, 2006) (Fig. 3). We recorded
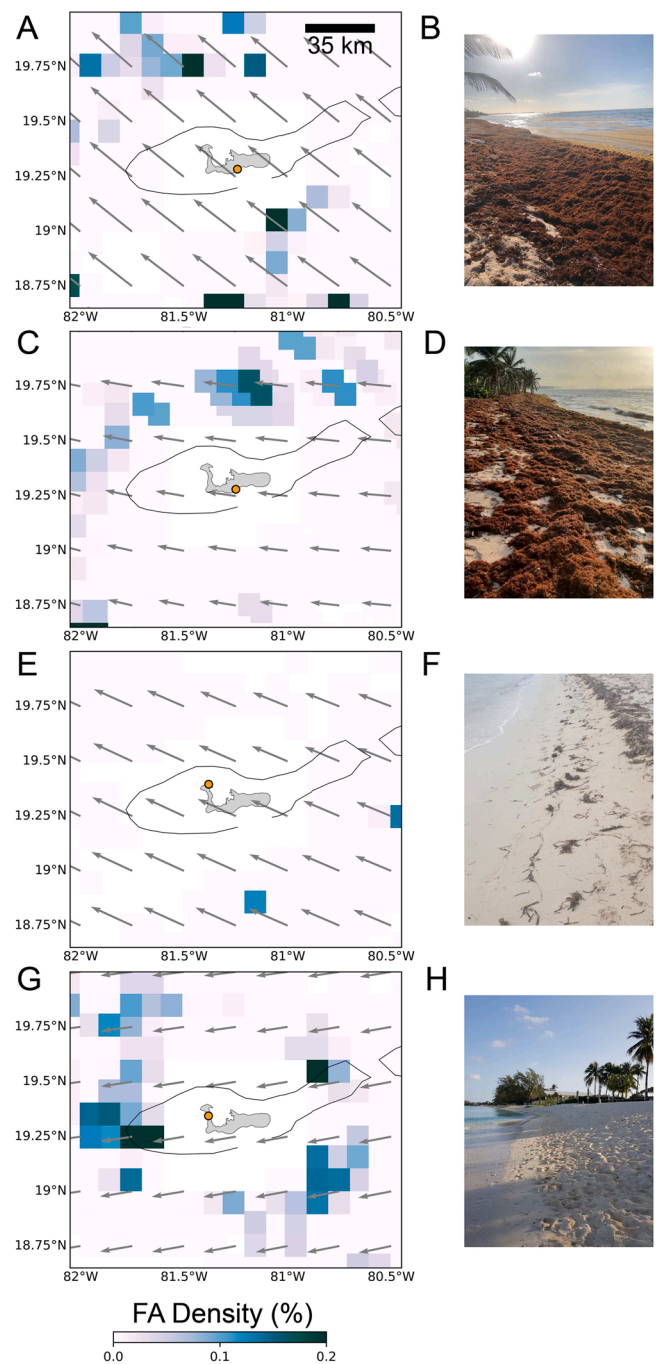
Fig. 2. Examples of FA density, wind velocity, and corresponding Sargassum Watch photos at Grand Cayman Island. Colored backgrounds show 7-day composite FA density values (white = no data available), grey arrows show the 7-day mean wind velocity, the orange circle shows the location of where the corresponding photo was taken, and the black contour line denotes the 1000 m water depth. Maps are Mercator projections, north is upward, the thick black scale bar in the upper corner of panel A shows a distance of 35 km. (A, B) On June 9, 2020, the observed site was 86% covered with Sargassum. The corresponding FA density = 0.4% and shoreward wind speed = 6.65 m/s. (C,D) On August 20, 2021, the observed site was 94% covered by Sargassum. The corresponding FA density = 0 and shoreward wind speed = 4.51 m/s. (E,F) On June 5, 2020, the observed site was 12% covered by Sargassum. The corresponding FA density = 0 and shoreward wind speed = −2.51 m/s. (G,H) On July 3, 2020 the observed site had 0% Sargassum. The corresponding FA density = 0.032% and shoreward wind speed = −5.33 m/s.
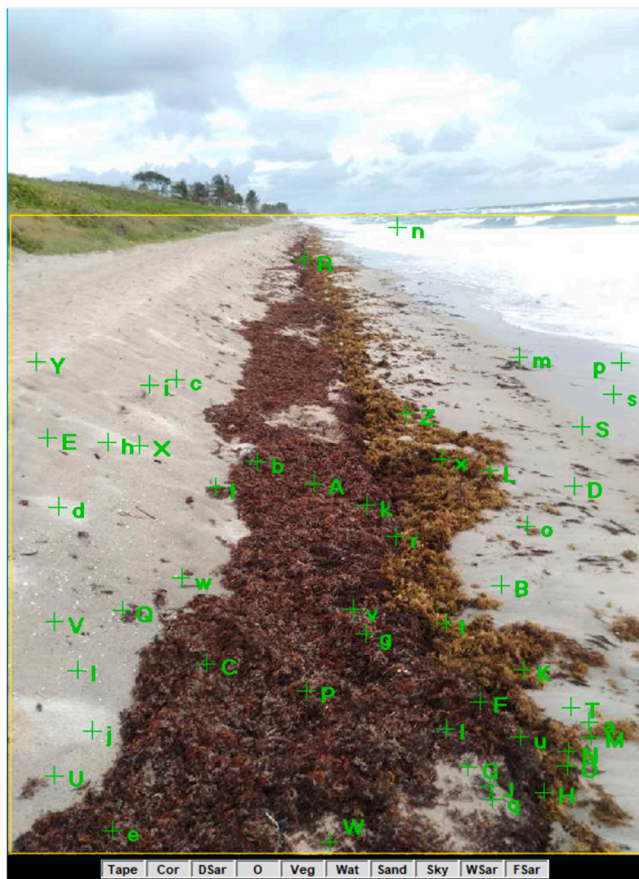
Fig. 3. Example of a Sargassum Watch photo, downloaded from the Epicollect5 platform that was processed using the Coral Point Counter with Excel extensions (Kohler and Gill, 2006). The yellow box shows how the photo was cropped to remove the sky; green crosses and corresponding letters indicate the locations of randomly distributed points where (at the central intersection) the location was designated as Sargassum, sand, sky, water, vegetation, or other. The percent coverage of Sargassum was determined by dividing the number of Sargassum points by the sum of points marking Sargassum, sand, water, and vegetation. This photo shows a site with 48% Sargassum coverage.

whether each point coincided with Sargassum, sand, sky, water, vegetation, or "other" (e.g., a person or beach furniture). To estimate the relative amount of Sargassum present (percent coverage), we divided the number of Sargassum points by the sum of sand, water, vegetation, and Sargassum points. Although slight differences in camera specifications and angles existed among uploaded photos from citizen scientists, such differences appeared to be random throughout the set of photos and were therefore deemed to be a minor introduction of noise into the subsequent analyses, rather than a source of bias that might skew statistical results.

2.1.2. Southeast Florida dataset

For the southeast Florida dataset we selected "Sargassum Watch" photos that had corresponding FA density and wind data and excluded photos where the metadata indicated evidence of site cleaning or where Sargassum was described as "mostly decomposed." This was done to identify photos that would best match the FA density values for a given week (i.e., excluding photos that were missing Sargassum because it had been removed due to site cleaning or photos that had Sargassum present from previous beaching events). Of the sites that met these criteria (Fig. 1B), we then attempted to select 10 photos for each month to produce a dataset with an even representation among years and seasons. However, not all months had at least 10 photos, hence slight differences in sample sizes existed among years (2019 = 76 photos, 2020 = 70

photos, 2021 = 73 photos) and among seasons (April – June = 80 photos, July – September = 82 photos, October- March = 57 photos). The percent coverage of Sargassum in each photo was obtained as described above.

2.1.3. Puerto Morelos dataset

Data were obtained from Rutten et al. (2021). In that study, hourly images were collected during daylight hours from two stationary cameras from September 2015 to November 2020 at Puerto Morelos beach, 30 km south of Cancun, Quintana Roo, Mexico (Fig. 1C). Cameras were mounted on land and oriented along the shoreline. The number of Sargassum mat "arrivals" (i.e., beaching) in every day were classified as "non-existent", "small", "medium", and "large" in a supervised manner to ensure accuracy (Rutten et al., 2021). To compare against the 7-day FA density index used in SIRs, we summed the hourly counts of Sargassum mats (irrespective of classified size) from the video data across the corresponding 7-day periods. These weekly counts were obtained between January 2019 and November 2020 (n = 97 weeks), overlapping with available SIR data.

2.2. Statistical analyses

For the regional and site-specific datasets, we designed our analysis to (1) examine the relationship between the FA density metric used in SIR risk values and in situ observation of Sargassum at the same sites, and (2) determine whether including wind data along with FA density could increase the correspondence. For each photo analyzed, we obtained the corresponding FA density and wind velocity associated with that coastal site. The FA density was a composite from the date of the picture extending to the previous 7-days, covering a fixed radius of 50 km from the shoreline with a mask between 0 and 30 km (Fig. 1D,E). The FA density for a given location is set as the maximum value within that 50 km radius (Triñanes et al., 2021). For wind velocities, we used the European Centre for Medium-Range Weather Forecasts (ECMWF) Reanalysis v.5 (ERA5) (Hersbach et al., 2020). Wind data were available at 10 m above sea level at hourly timesteps at a resolution of 30 km. For each of the citizen science photos that provided a latitude, longitude and date, we took the weighted average of hourly shoreward wind speed at the four closest grid points to a given coastal location (grid points closer to the coastal location were weighted more heavily than grid points more distant). In the analyses presented, shoreward wind velocity was positive and offshore wind velocity was negative. From these data we calculated the following wind speed metrics (see below regarding the time period over which these were calculated): (1) the mean shoreward wind speed, (2) the maximum shoreward wind speed, and (3) the minimum shoreward wind speed. We examined these three metrics to account for different aspects of nearshore wind dynamics, owing to lack of information on whether averaged wind conditions acting on Sargassum over time or the extremes in wind conditions (maximum/minimum) might be more important for influencing Sargassum beaching. Likewise, given that it was not possible to determine when the Sargassum observed in the photo washed ashore, there is uncertainty in what temporal range is most appropriate for the wind data. We tested three different time-lags: 0–1 days before, 0–3 days before, and 0–7 days before to the photo date (Fig. 1D). In analyses using data from Puerto Morelos, Quintana Roo, Mexico, we only considered 7-day metrics of wind velocity because the data were summarized as the number of mats per week. (Fig. 1E).

We used linear regressions to determine how much of the variance in Sargassum coverage (or number of Sargassum mats) observed could be accounted for by FA density and each of the wind metrics. Analyses were conducted separately for the region-wide dataset (436 sites), the southeast Florida, USA dataset (219 sites), and the Puerto Morelos dataset (97 weeks). We also examined whether there were differences among seasons in the relationships between FA density and wind velocity. To simplify this analysis, we selected the wind metric with the

strongest correlation for the full dataset to use in the seasonal comparisons. We chose three seasons in this analysis, spring: April-June (early, high pelagic *Sargassum* season), summer: July-September (late, high pelagic *Sargassum* season) and autumn/winter: October-March (low pelagic *Sargassum* season). In each of these analyses we report the Adjusted (Adj.) R^2 value to control for differences in the number of predictor variables included in the regressions. Finally, for the region-wide dataset we used the coefficients and their 95% Confidence Intervals (CI) from the linear regression model with the highest predictive ability to examine how wind velocity would influence the amount of *Sargassum* likely to be observed along the coastline. These predictions were made assuming there was no *Sargassum* detected offshore (FA density = 0.00%), at the transition point between "low" and "medium" risk (FA density = 0.05%), and at the transition point between "medium" and "high risk" (FA density = 0.20%).

3. Results

3.1. Comparing offshore FA density and wind metrics to observed coastal sargassum

3.1.1. Region-wide dataset

In the region-wide analysis, linear regressions indicated that offshore FA density was weakly but positively related to *Sargassum* coverage observed on the coast (Adj. R^2 = 0.035, p < 0.001, n = 436). Including any of the wind metrics greatly improved the variance in *Sargassum* coverage that could be accounted for (Table 1). In all cases, the higher the shoreward wind velocity was, the higher the percent coverage of *Sargassum* in the corresponding photo. Of the metrics examined, mean shoreward wind speed tended to account for more of the variance in *Sargassum* coverage than the maximum or minimum values over the

same time range (Table 1). Including the 7-day mean wind speed with FA density performed best (Adj. R^2 = 0.276, p < 0.001, n = 436) (Fig. 4). Similar performance was seen when including the 3-day mean wind speed (Adj. R^2 = 0.273, p < 0.001, n = 436) and the 1-day mean wind speed (Adj. R^2 = 0.264, p < 0.001, n = 436). The relationships detected combining FA density and the 7-day mean shoreward wind speed were also seen separately in each season (Table 2).

3.1.2. Southeast Florida dataset

In the site-specific case along southeast Florida, FA density was not correlated with observed *Sargassum* coverage on the coast (Adj. R^2 = 0.000, p > 0.05, n = 219). Including wind metrics improved the variance accounted for somewhat, with 3-day mean wind speed performing best (Adj. R^2 = 0.033, p = 0.01, n = 219) (Table 1). Examining seasonal differences in these relationships also indicated no relationship between offshore FA density and observed *Sargassum* coverage at the coast. However, including the 3-day mean wind speed significantly improved correlations in the spring and summer (when *Sargassum* is most abundant) although it did not improve correlations for autumn/winter (Table 2).

3.1.3. Puerto Morelos dataset

In the site-specific case at Puerto Morelos, FA density was positively related to the number of *Sargassum* mats reaching the coast (Adj. R^2 = 0.238, p < 0.001, n = 97). Including 7-day wind metrics of the minimum shoreward wind velocity improved correlations the most; the higher the minimum shoreward velocity over the course of the week, the more mats were expected to wash ashore. Examining seasonal differences in these relationships indicated that FA density was only significantly related to the number of *Sargassum* mats detected in summer. Including the minimum shoreward wind velocity greatly improved

Table 1

Relationships between offshore FA density/wind metrics and the amount of *Sargassum* observed along the coast. Adjusted R^2 are reported, values closer to 1 indicate that more of the variance in observations can be accounted for by the predictor variables. Whether FA density alone is a significant predictor of observations is denoted with crosses (p < 0.05 = +, p < 0.001 = ++), whether including a wind metric significantly increases the variance accounted for is denoted with asterisks (p < 0.05 = *, p < 0.001 = **). Results are shown for the region-wide analysis (n = 436 sites), southeast Florida, USA (n = 219 sites) and Puerto Morelos, Mexico (n = 97 weeks). The wind metric that most improved FA density predictions and that were subsequently used in the seasonal analysis (Table 2) for each of the datasets are highlighted in grey and in bold text.

	Regional (Adj. R^2)	SE FL (Adj. R^2)	Puerto Morelos (Adj. R^2)
FA density	0.035++	0.000	0.238++
+1d mean wind	0.264**	0.029**	--
+1d max wind	0.249**	0.030	--
+1d min wind	0.254**	0.022*	--
+3d mean wind	0.273**	**0.033****	--
+3d max wind	0.237**	0.014*	--
+3d min wind	0.244**	0.004	--
+7d mean wind	**0.276****	0.003	0.262*
+7d max wind	0.193**	-0.002	0.241
+7d min wind	0.216**	0.006	**0.325****
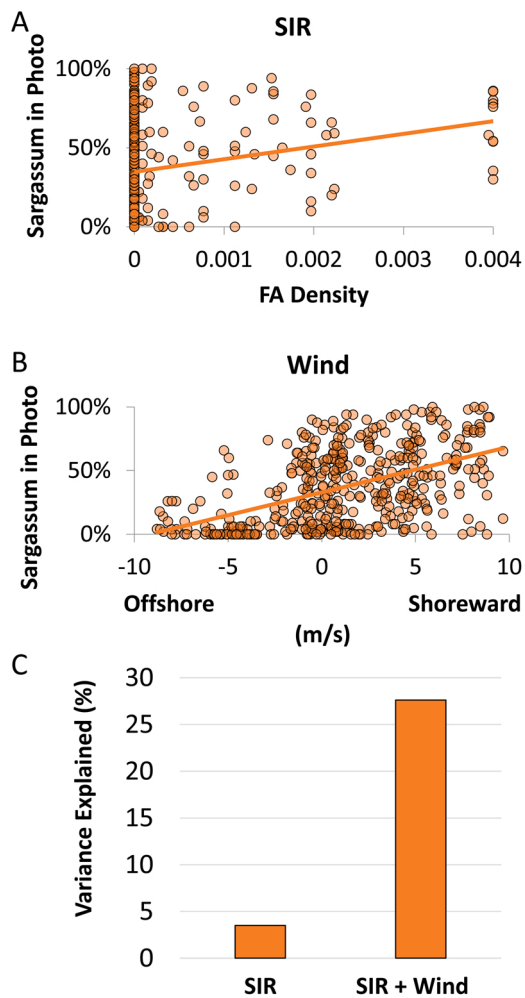
Fig. 4. Region-wide comparison of the percent coverage of coastline covered by *Sargassum* in photos to the corresponding (A) satellite-derived FA density of the nearest grid cell to the coastal site and (B) the 7-day mean shoreward wind velocity. (C) Adjusted R^2 values indicating how much variance in coastal coverage of *Sargassum* is explained by the offshore FA density used in the SIR risk estimates (SIR) and by the combination of FA density and the 7-day mean shoreward wind velocity (SIR + Wind).

Table 2

Seasonal relationships between offshore FA density/wind metrics and the amount of *Sargassum* observed along the coast (Adjusted R^2). For the regional dataset the 7-day mean shoreward wind speed was used, for southeast Florida the 3-day mean shoreward wind speed was used, and for Puerto Morelos the 7-day minimum shoreward wind speed was used. Other conventions as in Table 1.

Dataset	Season	FA density (Adj. R^2)	+ wind (Adj. R^2)	N
Regional	April – June	0.048 +	0.234 **	118
Regional	July – September	0.006	0.377 **	192
Regional	October – March	0.031 +	0.211 **	126
SE Florida	April – June	-0.012	0.156 **	80
SE Florida	July – September	-0.007	0.063 *	82
SE Florida	October – March	0.032	0.033	57
Puerto Morelos	April – June	-0.044	0.323 *	24
Puerto Morelos	July – September	0.430 ++	0.435	27
Puerto Morelos	October – March	-0.021	-0.041	46

correlations in spring but had little influence in summer or autumn/winter (Table 2). The continuous timeseries of the Puerto Morelos mat arrivals relative to the 7-day minimum shoreward wind speed and FA density similarly show a reasonable correspondence for the summer

months, but less consistent predictions for winter and spring months (Fig. 5).

3.2. Predicting regional sargassum coverage using FA density and wind speed

We used the results of the region-wide regression analyses (Fig. 4) to predict the amount of Sargassum that washes ashore across a range of wind speeds and FA densities (Fig. 6). The coefficient for FA density was 62.6 (95% CI = 29.22 – 95.98), 7-day mean shoreward wind speed was 0.0349 (95% CI = 0.0292 – 0.0406), and the intercept was 0.3145 (95% CI = 0.224 – 0.325). We plotted the predicted percent coverage of beached Sargassum using FA densities of 0.00% (no Sargassum detected offshore), 0.05% (the transition between "low" and "medium" risk in the SIR), and 0.2% (the transition between "medium" and "high" risk in the SIR) for wind speeds ranging from − 10 to + 10 m/s. Winds appear to play a considerable role in the amount of predicted Sargassum coverage of a beach. At an FA density of 0.00%, winds blowing shoreward at a mean value of 5 m/s are predicted to result in 43–54% of the beach being covered in Sargassum, whereas if winds were 5 m/s offshore 8–19% of the beach is predicted to be covered (Fig. 6A). When offshore FA densities = 0.05% (the SIR "medium risk" threshold) and winds are blowing in a shoreward direction at a mean value of 5 m/s, ~45–59% of the beach might be expected to be covered by Sargassum. In contrast, if winds were blowing away from shore at 5 m/s, only 10–24% of the beach would be expected to be covered by Sargassum (Fig. 6B). Similarly, at FA densities = 0.2% (the SIR "high risk" threshold), shoreward winds of 5 m/s would be expected to result in 49–74% beach coverage whereas with the same FA density but winds blowing away from shore at 5 m/s only 14–38% of the beach is predicted to be covered by Sargassum (Fig. 6C).

4. Discussion

Our analysis indicates that offshore FA densities used in SIRs are only weakly related to observations by citizen scientists at corresponding coastal sites across the region. There are several methodological factors that may confound detecting a strong relationship between these two datasets (e.g., non-standardized photos and possible mismatches between when photos were taken, when Sargassum washed ashore, and the timing and accuracy of composite satellite imagery). Even so, for our analysis, including concurrent wind metrics dramatically improved the agreement, suggesting that part of the discordance between offshore FA densities and Sargassum observed on the coast is due to not accounting for the movement of Sargassum. The analyses were not particularly sensitive to how shoreward wind was quantified; for each of the three datasets the differences in the variance explained by the "best" and "worst" performing wind metric was less than 8.5% (Table 1). Our region-wide regression analyses, in particular, indicate that the amount of Sargassum observed on the beach is highly dependent on wind conditions and was robust to a wide range of assumptions related to the temporal aspects of wind metrics and seasons (Tables 1 and 2).

We expect that including shoreward wind velocities could be especially useful in refining SIR risk estimates. As an example, in the case of small islands, in scenarios where the amount of Sargassum offshore may be high around the entire island, under the current SIR algorithm, inundation risk would be considered high along the island's entire coastline. We hypothesize that, in reality, inundation of Sargassum would be less likely on the leeward side of the island compared to the windward side (Fig. 2). Such differences would be reflected in risk estimates if shoreward wind velocities were incorporated into the SIR algorithm. For example, even with the same amount of Sargassum detected offshore, the percentage of the beach predicted to be covered ranges from 0 to ≥ 75%, depending on the shoreward wind velocity (Fig. 6). Uncertainty in beach coverage predictions increases when higher FA density is detected offshore. At the highest FA densities
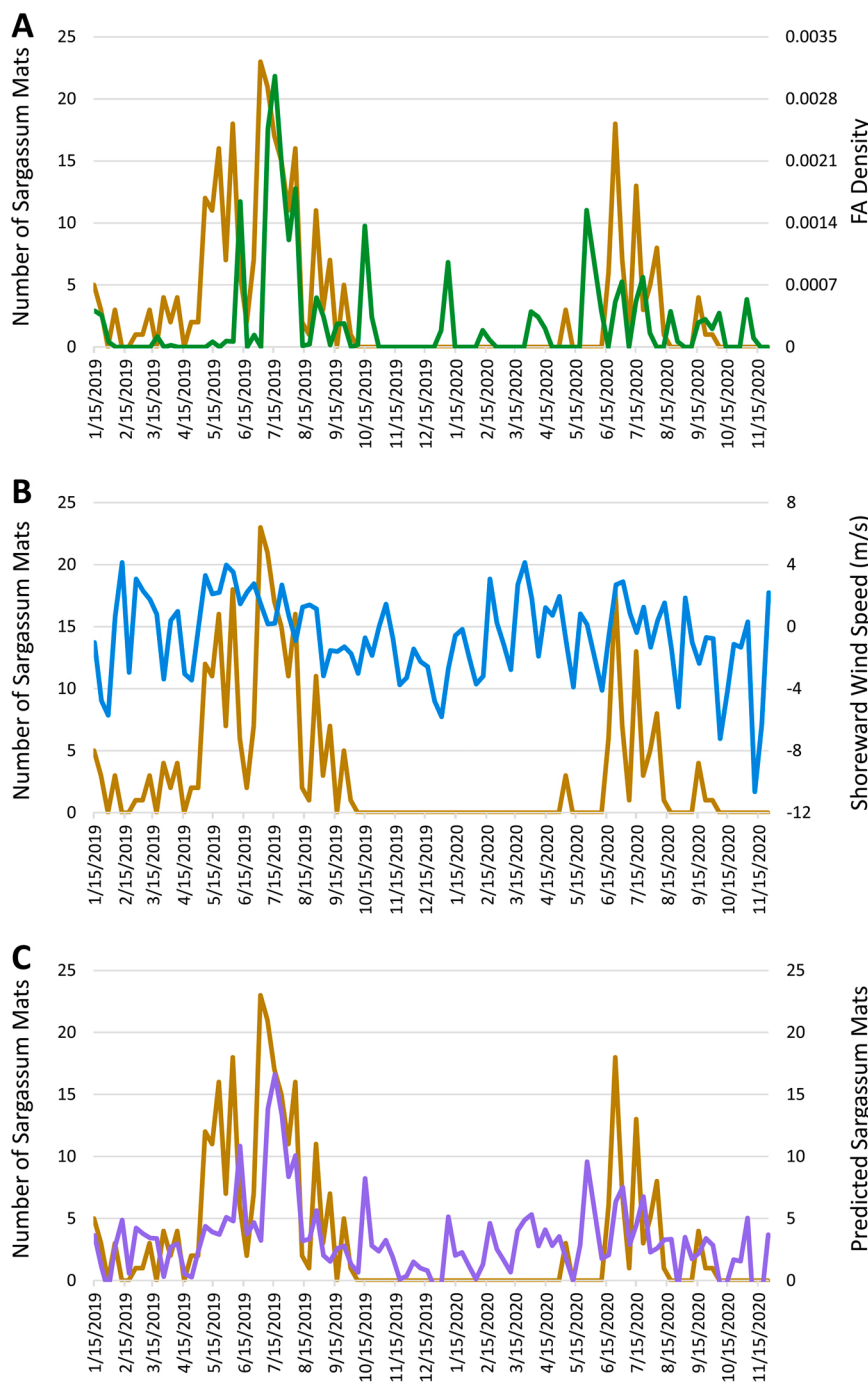
Fig. 5. Timeseries showing the number of Sargassum mats arriving to Puerto Morelos, Mexico (gold line) relative to (A) 7-day composite Floating Algal (FA) density used in the Sargassum Inundation Reports (green line); (B) the minimum shoreward wind speed over the 7-day period, positive values = onshore, negative values = offshore (blue line); and (C) the predicted number of Sargassum mats based on the regression model using the combination of FA density and wind speed (purple line). Annual variance explained in Sargassum mats arriving are shown in Table 1 and seasonal variance explained is shown in Table 2.

detected (~0.4%) and 5 m/s shoreward windspeed, Sargassum is predicted to cover between 55% and 93% of the beach. Under the same wind conditions and an FA density threshold for "medium risk" (0.05%), 45–59% of the beach is predicted to be covered. These findings point to the value of including wind-driven dynamics into SIR risk estimates.

Interestingly, when wind velocities average 0 m/s and FA density is 0.00%, there is still predicted to be 31% (28–34%) Sargassum coverage on the beach (Fig. 6A). This may imply that offshore FA densities tend to be underestimates of the amount of Sargassum in the vicinity of the coastline. This is not entirely unexpected given that a large swath of ocean (0–30 km) is not depicted in the FA density index and smaller patches of Sargassum go undetected by satellite (see below). Additionally, however, this may also suggest a bias in observers being more likely to take photos when Sargassum is present than when coastal areas are

clear. Possible bias in validation data will be important to consider when working to improve SIR risk estimates with wind data.

Likewise, site-specific analyses suggest that some care is warranted in this application and for expectations that this simple addition will bring about complete correspondence between risk estimates and Sargassum beaching. Despite our attempts to select photos best suited for comparison to offshore FA densities in southeast Florida, there was no relationship between offshore detections of Sargassum and what was observed on the beach. Including wind in the regression analysis only had a modest positive influence in improving correspondence. In contrast, at Puerto Morelos, the FA densities alone performed reasonably well in accounting for the number of incoming Sargassum mats. Wind metrics did improve the correspondence between observations, but not as much as was seen in the region-wide analysis. The difference between
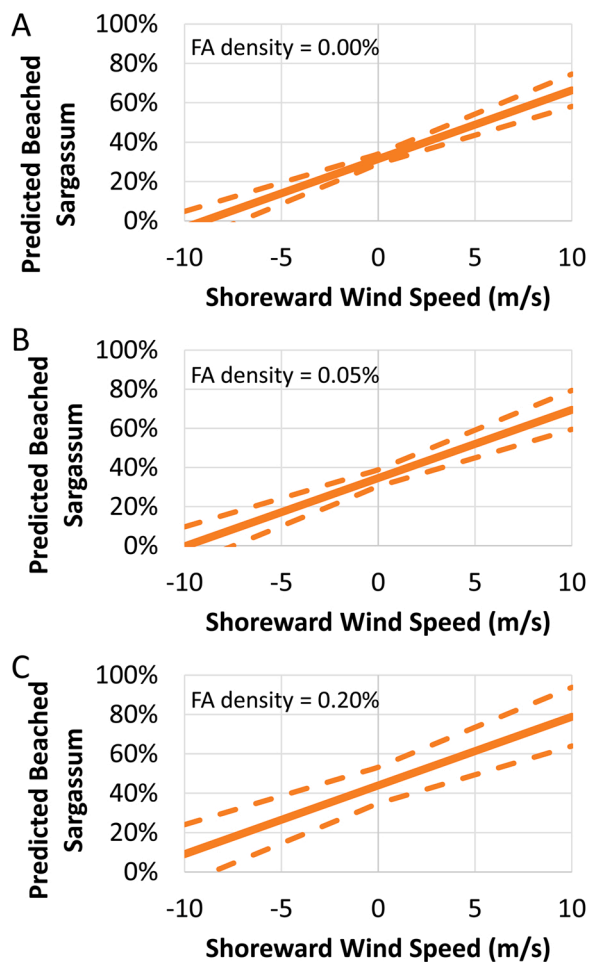
Fig. 6. Predictions of the amount of beached Sargassum (% coverage, y-axis) assuming different 7-day mean shoreward wind velocities (negative = offshore, positive = onshore, x-axis). The range of wind speeds plotted corresponds to the range observed in the regional dataset (n = 436 sites). Solid lines are based on the estimated coefficients for FA density and wind velocity, dashed lines correspond to the 95% CI. (A) Results assuming FA density = 0.00%, no Sargassum detected offshore. (B) Results assuming FA density = 0.05%, the threshold for "medium" Sargassum inundation risk. (C) Results assuming FA density = 0.20%, the threshold for "high" Sargassum inundation risk.

these two sites may be attributable, in part, to how Sargassum was monitored (i.e., in Puerto Morelos the data were collected continuously and in a more standardized manner). However, it is likely that differences are not just due to how Sargassum at the coast was quantified.

The factors besides wind that influence Sargassum beaching are numerous (e.g., currents, waves, tidal regime, bathymetry, and coastal geomorphology), and their interactions are complex and are likely weighted differently depending on the physical setting (Chávez et al., 2020; Rutten et al., 2021). For instance, unlike other coastal areas monitored, surface currents within < 20 km of the southeast Florida coast travel northwards at upwards of 80 km per day. This may introduce considerable discrepancies between FA densities summed over a 7-day period and the wind conditions at that location. For southeast Florida, 7-day composites of FA density from offshore locations further south may be more representative of beaching risk at a given stretch of coastline rather than locations immediately adjacent to it. Future work could explore varying the radius over which composite FA densities are calculated according to surrounding ocean current velocity. In all cases, there is a gap in available wind, wave, and current data to estimate the final movements of Sargassum within ~10 km from the coast and to predict if, when, and where it will wash ashore. Without resolving this

aspect of Sargassum movement, high variance and uncertainty in predicted Sargassum beaching is likely. Another source of variance may result from the proportion of Sargassum morphotypes differing between sites (Iporac et al., 2022). In principle, the different morphological characteristics could influence their movement (García-Sánchez et al., 2020; Magaña-Gallegos et al., 2022), and thus the response of Sargassum to physical factors could differ also (Beron-Vera and Miron, 2020).

This complexity in predicting Sargassum beaching can also be inferred from the seasonal analyses conducted here. While seasonal relationships between FA density/wind velocity and Sargassum observations at the coast were consistent at the regional scale, this was not the case for either site-specific dataset. For both southeast Florida and Puerto Morelos, FA density was unrelated to Sargassum observations at the coast during the spring, and including wind metrics greatly improved correlations. In summer, however, shoreward wind speed marginally improved predictions of beached Sargassum in southeast Florida, whereas at Puerto Morelos, FA density alone was a strong predictor of beaching Sargassum. In the autumn/winter, neither FA density nor wind speed accounted for Sargassum beaching at either location. It is encouraging that during the main Sargassum season (spring and summer) the combination of offshore FA density, and therefore present SIR assessments, and wind speed can reasonably account for Sargassum observed along the coast. However, the discrepancies between sites suggest that more complex algorithms that account for differences in the physical setting may be needed to fine-tune inundation risk estimates at smaller scales more practical for site-specific management, for example by using high-resolution satellite data collected over nearshore waters (Zhang et al., 2022) and numerical models tailored for nearshore applications (Liu et al., 2020).

The satellite-derived FA density maps are subject to large uncertainties over coastal waters due to medium resolution and algorithm imperfection, which leads to a data gap for waters within 30 km of the shoreline (Fig. 2) and possible underestimates of Sargassum in offshore waters due to small Sargassum mats that are not detected by the satellites. For example, the detection limit from the medium-resolution satellite data is 0.2% of a pixel size (Wang and Hu, 2016; i.e., if all Sargassum mats within an image pixel have an integrated size of < 0.2% of a pixel, then they are not detectable). These uncertainties may lead to variable relationships between the satellite-detected offshore Sargassum amount and the beaching amount. For example, while the Sargassum amount removed from beaches of Fort Lauderdale (Florida, USA) correlated with region-wide satellite observations in offshore waters (Fig. 4e of Tomenchok et al., 2021), such correspondence was not observed along beaches on the northern Mexican Caribbean (Fig. 4 of Rodriguez-Martinez et al., 2022). In the future, the 30-km nearshore mask may be reduced to 10 km by using a new machine learning algorithm applied to the same medium-resolution data (Hu et al., 2023), and uncertainties due to the use of medium-resolution data may be minimized through the use of fine-resolution satellite data and better algorithms (Cuevas et al., 2018; Wang and Hu, 2021). For example, Zhang et al. (2022) showed greatly improved monitoring capacity on beaches and nearshore waters using high-resolution commercial satellites, which could potentially be operationalized in future monitoring efforts and progressive iterations of SIR risk estimates. The temporal resolution can also be improved through the use of multi-sensor satellite data as clouds (a normal visually limiting factor) are not persistent in one location. Similarly, improving consistency of citizen science monitoring programs, rather than full reliance on opportunistic data contributions, could aid in directly linking satellite, wind and in situ observations. For example, capitalizing on existing systematic monitoring programs might be especially useful contributions to the "Sargassum Watch" citizen science program, thereby providing more regular, standardized observations of beached Sargassum (Arellano-Verdejo et al., 2021; Marsh et al., 2021; Hernández et al., 2023). Additionally, expanded continual video monitoring, such as used by Rutten et al. (2021) in the Puerto

Morelos dataset, may offer benefits to Sargassum beaching validation in additional locations. Ultimately, reducing the uncertainties between offshore algal detection and Sargassum beaching events will require the combination of multiple approaches.

The complexities noted above point to the challenges of understanding the spatial ecology of pelagic Sargassum. Our work is a step towards quantifying the role and implications of wind-driven movement of Sargassum from open ocean habitats into coastal areas. Improvement of region-wide SIR risk assessments are likely to be achieved by including shoreward wind velocities into existing algorithms. These findings are in line with other studies that have shown the importance of considering wind effects on the movement and distribution of Sargassum (Putman et al., 2020; Berline et al., 2020; Beron-Vera et al., 2022). It is also worth considering that, because both FA densities and wind data are taken offshore, there may be utility in examining whether SIRs could provide short-term (~1 week) forecasts of inundation risk to supplement their use as a monitoring tool. Future work in this area as well as considering other aspects that influence the transport of Sargassum such as ocean currents, waves, and the inertial effects associated with specific Sargassum morphotypes deserve prioritization (Brooks et al., 2019; Beron-Vera and Miron, 2020; Triñanes et al., 2022; Putman and Hu, 2022).

Declaration of Competing Interest

The authors declare that they have no known competing financial interests or personal relationships that could have appeared to influence the work reported in this paper.

Data Availability

Data will be made available on request.

References

Arellano-Verdejo, J., Lazcano-Hernández, H.E., 2021. Collective view: mapping Sargassum distribution along beaches. PeerJ Comput. Sci. 7, e528.

Berline, L., Ody, A., Jouanno, J., Chevalier, C., André, J.M., Thibaut, T., Ménard, F., 2020. Hindcasting the 2017 dispersal of Sargassum algae in the Tropical North Atlantic. Mar. Pollut. Bull. 158, 111431.

Bernard, D., Biabiany, E., Cécé, R., Chery, R., Sekkat, N., 2022. Clustering analysis of the Sargassum transport process: application to beaching prediction in the Lesser Antilles. Ocean Sci. 18 (4), 915–935.

Beron-Vera, F.J., Miron, P., 2020. A minimal Maxey–Riley model for the drift of Sargassum rafts. J. Fluid Mech. *904*.

Beron-Vera, F.J., Olascoaga, M.J., Putman, N.F., Triñanes, J., Lumpkin, R., Goni, G., 2022. Dynamical geography and transition paths of Sargassum in the tropical Atlantic. AIP Adv. 12, 105107.

Brooks, M.T., Coles, V.J., Coles, W.C., 2019. Inertia influences pelagic sargassum advection and distribution. Geophys. Res. Lett. 46 (5), 2610–2618.

Chávez, V., Uribe-Martínez, A., Cuevas, E., Rodríguez-Martínez, R.E., van Tussenbroek, B.I., Francisco, V., Estévez, M., Celis, L.B., Monroy-Velázquez, L.V., Leal-Bautista, R., Álvarez-Filip, L., 2020. Massive influx of pelagic Sargassum spp. on the coasts of the Mexican Caribbean 2014–2020: challenges and opportunities. Water 12 (10), 2908.

Cuevas, E., Uribe-Martínez, A., Liceaga-Correa, M.D.L.Á., 2018. A satellite remote-sensing multi-index approach to discriminate pelagic Sargassum in the waters of the Yucatan Peninsula, Mexico. Int. J. Remote Sens. 39 (11), 3608–3627.

Cunha, D.G.F., Casali, S.P., de Falco, P.B., Thornhill, I., Loiselle, S.A., 2017. The contribution of volunteer-based monitoring data to the assessment of harmful phytoplankton blooms in Brazilian urban streams. Sci. Total Environ. 584–594.

Dassié, E.P., Gourves, P.Y., Cipolloni, O., Pascal, P.Y., Baudrimont, M., 2022. First assessment of Atlantic open ocean Sargassum spp. metal and metalloid concentrations. Environ. Sci. Pollut. Res. 29 (12), 17606–17616.

Devault, D.A., Modestin, E., Cottereau, V., Vedie, F., Stiger-Pouvreau, V., Pierre, R., Coynel, A., Dolique, F., 2021. The silent spring of Sargassum. Environ. Sci. Pollut. Res. 28 (13), 15580–15583.

Franks, J.S., Johnson, D.R., Ko, D.S., 2016. Pelagic sargassum in the tropical North Atlantic. *Gulf and Caribbean.* Research 27 (1), SC6–SC11.

García-Sánchez, M., Graham, C., Vera, E., Escalante-Mancera, E., Álvarez-Filip, L., van Tussenbroek, B.I., 2020. Temporal changes in the composition and biomass of beached pelagic Sargassum species in the Mexican Caribbean. Aquat. Bot. 167, 103275.

Geldmann, J., Heilmann-Clausen, J., Holm, T.E., Levinsky, I., Markussen, B., Olsen, K., Rahbek, C., Tøttrup, A.P., 2016. What determines spatial bias in citizen science? Exploring four recording schemes with different proficiency requirements. Divers. Distrib. 22, 1139–1149.

Gillis, C.-A., Dugdale, S.J., Bergeron, N.E., 2018. Effect of discharge and habitat type on the occurrence and severity of *Didymosphenia 20eminate* mats in the Restigouche River, Eastern Canada: Effect of discharge and habitat type on the severity of *D. 20eminate.* Ecohydrology 11, e1959.

Hernández, H.E.L., Arellano-Verdejo, J., Romero, M.S., 2023. Acciones colaborativas para el monitoreo del sargazo. Ecofronteras 8–12.

Hersbach, H., Bell, B., Berrisford, P., Hirahara, S., Horányi, A., Muñoz-Sabater, J., Nicolas, J., Peubey, C., Radu, R., Schepers, D., Simmons, A., 2020. The ERA5 global reanalysis. Q. J. R. Meteorol. Soc. 146 (730), 1999–2049.

Hu, C., Murch, B., Barnes, B.B., Wang, M., Maréchal, J.P., Franks, J., Johnson, D., Lapointe, B., Goodwin, D., Schell, J., Siuda, A., 2016. Sargassum watch warns of incoming seaweed. Eos 97 (22), 10–15.

Hu, C., Zhang, S., Barnes, B.B., Xie, Y., Wang, M., Cannizzaro, J.P., English, D.C., 2023. Mapping and quantifying pelagic Sargassum in the Atlantic Ocean using multi-band medium-resolution satellite data and deep learning. Remote Sens. Environ. 289, 113515.

Iporac, L.A.R., Olszak, S., Burkholder, D., Collado-Vides, L., 2020. Lessons and Challenges in Piloting "Sargassum Watch," A Citizen Science Program to Monitor Pelagic Sargassum Landings in South Florida. *Proceedings of the 72nd Gulf and Caribbean Fisheries Institute, November 2 - 8,* 2019 Punta Cana, Dominican Republic, pp. 246–252.

Iporac, L.A.R., Hatt, D.C., Bally, N.K., Castro, A., Cardet, E., Mesidor, R., Olszak, S., Duran, A., Burkholder, D.A., Collado-Vides, L., 2022. Community-based monitoring reveals spatiotemporal variation of sargasso inundation levels and morphotype dominance across the Caribbean and South Florida. Aquat. Bot. 182, 103546.

Johnson, D.R., Franks, J.S., Oxenford, H.A., Cox, S.A.L., 2020. Pelagic Sargassum prediction and marine connectivity in the tropical Atlantic. Gulf Caribb. Res. 31 (1), GCFI20–GCFI30.

Kohler, K.E., Gill, S.M., 2006. Coral Point Count with Excel extensions (CPCe): A Visual Basic program for the determination of coral and substrate coverage using random point count methodology. Comput. Geosci. 32 (9), 1259–1269.

Liu, Y., Weisberg, R.H., Zheng, L., 2020. Impacts of hurricane Irma on the circulation and transport in Florida Bay and the Charlotte Harbor estuary. Estuaries and Coasts 43, 1194–1216.

Lopez Miranda, J.L., Celis, L.B., Estévez, M., Chávez, V., van Tussenbroek, B.I., Uribe-Martínez, A., Cuevas, E., Rosillo Pantoja, I., Masia, L., Cauich-Kantun, C., Silva, R., 2021. Commercial potential of pelagic Sargassum spp. in Mexico. Front. Mar. Sci. 1692.

Magaña-Gallegos, E., García-Sánchez, M., Graham, C., Olivos-Ortiz, A., Siuda, A.N., van Tussenbroek, B.I., 2022. Growth rates of pelagic Sargassum species in the Mexican Caribbean. Aquat. Bot., 103614

Maréchal, J.P., Hellio, C., Hu, C., 2017. A simple, fast, and reliable method to predict Sargassum washing ashore in the Lesser Antilles. Remote Sens. Appl.: Soc. Environ. 5, 54–63.

Marsh, R., Addo, K.A., Jayson-Quashigah, P.N., Oxenford, H.A., Maxam, A., Anderson, R., Skliris, N., Dash, J., Tompkins, E.L., 2021. Seasonal predictions of holopelagic Sargassum across the tropical Atlantic accounting for uncertainty in drivers and processes: the SARTRAC ensemble forecast system. Front. Mar. Sci. 1417.

Millar, E.E., Hazell, E.C., Melles, S.J., 2019. The 'cottage effect' in citizen science? Spatial bias in aquatic monitoring programs. Int. J. Geogr. Inf. Sci. 33, 1612–1632.

Miron, P., Olascoaga, M.J., Beron-Vera, F.J., Putman, N.F., Triñanes, J., Lumpkin, R., Goni, G.J., 2020. Clustering of marine-debris-and Sargassum-like drifters explained by inertial particle dynamics. Geophys. Res. Lett. 47 (19) e2020GL089874.

Nerbonne, J.F., Ward, B., Ollila, A., Williams, M., Vondracek, B., 2008. Effect of sampling protocol and volunteer bias when sampling for macroinvertebrates. J. North Am. Benthol. Soc. 27 (3), 640–646.

Ody, A., Thibaut, T., Berline, L., Changeux, T., André, J.M., Chevalier, C., Blanfune, A., Blanchot, J., Ruitton, S., Stiger-Pouvreau, V., Connan, S., 2019. From In Situ to satellite observations of pelagic Sargassum distribution and aggregation in the Tropical North Atlantic Ocean. PLoS One 14 (9), e0222584.

Ortega-Flores, P.A., Serviere-Zaragoza, E., De Anda-Montañez, J.A., Freile-Pelegrín, Y., Robledo, D., Méndez-Rodríguez, L.C., 2022. Trace elements in pelagic Sargassum species in the Mexican Caribbean: identification of key variables affecting arsenic accumulation in S. fluitans. Sci. Total Environ. 806, 150657.

Oxenford, H.A., Cox, S.A., van Tussenbroek, B.I., Desrochers, A., 2021. Challenges of turning the Sargassum crisis into gold: current constraints and implications for the Caribbean. Phycology 1 (1), 27–48.

Putman, N.F., Hu, C., 2022. Sinking Sargassum. Geophys. Res. Lett. 49 (17) e2022GL100189.

Putman, N.F., Lumpkin, R., Olascoaga, M.J., Triñanes, J., Goni, G.J., 2020. Improving transport predictions of pelagic Sargassum. J. Exp. Mar. Biol. Ecol. 529, 151398.

Rodriguez-Martinez, R.E., Jordan-Dahlgren, E., Hu, C., 2022. Spatio-temporal variability of pelagic Sargassum landings on the northern Mexican Caribbean. Remote Sens. Appl.: Soc. Environ. 27, 100767.

Rutten, J., Arriaga, J., Montoya, L.D., Mariño-Tapia, I.J., Escalante-Mancera, E., Mendoza, E.T., van Tussenbroek, B.I., Appendini, C.M., 2021. Beaching and natural removal dynamics of pelagic Sargassum in a fringing-reef lagoon. J. Geophys. Res.: Oceans 126 (11) e2021JC017636.

Tomenchok, L.E., Abdool-Ghany, A.A., Elmir, S.M., Gidley, M.L., Sinigalliano, C.D., Solo-Gabriele, H.M., 2021. Trends in regional enterococci levels at marine beaches and correlations with environmental, global oceanic changes, community populations, and wastewater infrastructure. Sci. Total Environ. 793, 148641.

Triñanes, J., Putman, N.F., Goni, G., Hu, C., Wang, M., 2021. Monitoring pelagic Sargassum inundation potential for coastal communities. J. Oper. Oceanogr. 287, 1–12.

Triñanes, J., Hu, C., Putman, N.F., Olascoaga, M.J., Beron-Vera, F.J., Zhang, S., Goni, G. J., 2022. An integrated observing effort for sargassum monitoring and warning in the Caribbean Sea, Tropical Atlantic, and Gulf of Mexico. Oceanography 34 (4), 68–69.

Valentini, N., Balouin, Y., 2020. Assessment of a smartphone-based camera system for coastal image segmentation and Sargassum monitoring. J. Mar. Sci. Eng. 8, 23.

Wang, M., Hu, C., 2016. Mapping and quantifying Sargassum distribution and coverage in the Central West Atlantic using MODIS observations. Remote Sens Environ. 183, 350–367.

Wang, M., Hu, C., 2018. On the continuity of quantifying floating algae of the Central West Atlantic between MODIS and VIIRS. Int J. Remote Sens 39, 3852–3869.

Wang, M., Hu, C., 2021. Satellite remote sensing of pelagic Sargassum macroalgae: the power of high resolution and deep learning. Remote Sens. Environ. 264, 112631 https://doi.org/10.1016/j.rse.2021.112631.

Wang, M., Hu, C., Barnes, B.B., Mitchum, G., Lapointe, B., Montoya, J.P., 2019. The Great Atlantic Sargassum Belt. Science 365, 83–87.

Zhang, S., Hu, C., Barnes, B.B., Harrison, T.N., 2022. Monitoring Sargassum inundation on beaches and nearshore waters using planetscope/dove observations. IEEE Geosci. Remote Sens. Lett. 19, 1503605. https://doi.org/10.1109/LGRS.2022.3148684.